Effect of melting and electron-phonon coupling on the collapse of depleted zones in copper, nickel, and α-iron

V. G. Kapinos
Department of Radiation Materials Science, Russian Research Centre "Kurchatov Institute," Moscow 123182, Russia

D. J. Bacon
Department of Materials Science and Engineering, The University of Liverpool, P. O. Box 147, Liverpool L69 3BX, United Kingdom
(Received 5 September 1995)

Previous work has shown that the nucleation of a vacancy loop by collapse of a displacement cascade is possible when the depleted zone (DZ) can melt and crystallize during the thermal spike stage. In this paper calculations based on molecular-dynamics (MD) simulations of Cu, Ni, and Fe have been performed to investigate the influence on the melting and loop formation of the average vacancy concentration $\langle C_v \rangle$ and number of vacancies, N_v, in the DZ. It is demonstrated that collapse of the DZ is possible at a fixed value of $\langle C_v \rangle$ only for conditions where N_v exceeds a critical number $N_v^{\rm cr}$. Values of $N_v^{\rm cr}$ have been estimated and found to be in good agreement with ones obtained from fitting our previous theoretical calculations to the experiments. The strong electron-phonon coupling (EPC) in Ni influences the vacancy loop yield through the formation of an amorphouslike core in the DZ. The influence of the size of the DZ and $\langle C_v \rangle$ on the amorphization process has been investigated. The dependence of the amorphization temperature on the size of the DZ has been obtained. It has been shown that a DZ with small diameter (less than $2a_0$, where a_0 is the lattice parameter) cannot become amorphous in Ni even for $\langle C_v \rangle$ more than 20–30 at. % and initial temperatures above 5000 K. The DZ in iron does not melt and produce a vacancy loop if the EPC is taken to have the same value as Ni. A reduction by a factor of 2 in the strength of the EPC leads to the formation of melted regions and amorphous cores in the DZ in this metal. In reality, however, the EPC strength for Fe is believed to be higher than for Ni, which means that the very low yield of vacancy loops in Fe compared to Ni can be explained by the low probability for the DZ to melt in the thermal spike.

I. INTRODUCTION

It has been shown by molecular dynamics (MD) that the core of a displacement cascade can pass through a vacancy-rich liquidlike phase while the thermal spike develops.[1,2] During crystallization of this melted core, vacancies are swept to the center by the advance of the solid/liquid interface.[3,4] As a result, a zone is formed where the average concentration of vacancies is several times larger than that before the onset of the thermal spike phase. Such zones are unstable and may collapse to form vacancy clusters such as dislocation loops. The physics of this effect has been the subject of many papers.[5–11]

We have recently developed a model[11] that is an extension of that described in Refs. 8 and 12. It simulates the process of heat propagation in the cascade damage region, including absorption and creation of latent heat, melting, and the redistribution of density within the melt under the influence of the temperature gradient. We refer to this model as "hybrid" because the continuum approximation, based on the solution of the partial differential equation of heat conduction, is used to describe the thermal spike stage, after the initial defect and temperature distributions are calculated by the MARLOWE code.[13] According to this model, a vacancy loop is produced in such a zone when both the average concentration of vacancies, $\langle C_v \rangle$, and their total number $\langle N_v \rangle$ exceed critical values $C_v^{\rm cr}$ and $N_v^{\rm cr}$, respectively. However, if $\langle C_v \rangle$ and $\langle N_v \rangle$ exceed some value $C_v^{\rm am}$ and $N_v^{\rm am}$ during the cooling under the influence of strong electron-phonon coupling (EPC), for instance, in metals such as Ni and Fe, the melted zone cannot crystallize completely and solidifies to a solid with a structure akin to an amorphous zone, which prevents collapse to a vacancy loop. The values of $C_v^{\rm cr}$, $C_v^{\rm am}$, $N_v^{\rm cr}$, and $N_v^{\rm am}$ can be extracted from comparison of vacancy loop yield and cascade efficiency calculated from the model with trends in experimental data obtained from ion-irradiated foils.

We use the word "amorphous" rather loosely here and do not claim the material is amorphous in a strict sense. In fact, we have made no attempt to analyze this structure in detail because it is small and strongly affected by the surrounding crystal. It will be seen that this region has a high concentration of vacancies dispersed within it and a large fraction of the remaining atoms are far from lattice sites. We use the term amorphous to distinguish this structure from that of a "collapsed" core, where the atoms occupy sites associated with the strain field of extended defects such as dislocation loops and stacking fault tetrahedra in a lattice.

It was demonstrated in Ref. 11 that in Cu about half of the cascades having an average concentration of vacancies in the depleted zone (DZ) at the end of the thermal stage of more than 3–4 at. % can produce experimentally visible vacancy loops if the average number of vacancies in such collapsed zones is more than about 60. For Ni, on the other hand, the strong EPC reduces the lifetime of the molten zone and can produce depleted zones with $\langle C_v \rangle$ of more than 20 at. %. The rapid cooling of the melt freezes the disordered structure

within the solidified DZ. Comparison of the calculations with experiments has demonstrated[11] that the best agreement between calculated and experimental yields in Ni can be achieved for $C_v^{\rm am}=21-22$ at. % and $N_v^{\rm am}=25$.

The numerical estimation of the critical cascade parameters using the hybrid model is not based on direct atomic-scale simulations of cascades, however. To investigate their physical basis further and assess the estimates of their values, it is important to use the alternative approach based purely on the MD method. In this paper, therefore, the basic mechanism of DZ collapse in metals with different strength of EPC has been investigated using the MD method. The emphasis has been to investigate the physical nature of the model critical parameters $C_v^{\rm cr}$ and $N_v^{\rm cr}$ in Cu and $C_v^{\rm am}$ and $N_v^{\rm am}$ in Ni. Fe also has been considered as an example of a metal with very strong EPC. All calculations have been conducted by employing a simplified version of the two-dimensional (2D) thermal spike model based on the MD code.

II. MODEL

For this work we have considered fcc (Cu,Ni) and bcc (Fe) metals. We have used the many-body interatomic potentials for these metals derived in Ref. 14, but modified as described in Ref. 15 to reproduce the pressure-volume relationships of single crystals and to provide better treatment of interactions inside the normal nearest-neighbor distance.

The energy relaxation process was simulated in a rectangular calculation cell extended along the x and y axes with dimensions $60a_0\times60a_0\times2a_0$ and consisting of 44 652 (fcc lattice) and 22 326 (bcc lattice) movable atoms. The cell had rigid boundary conditions along x and y and a periodic one along the z axis. Some atoms were randomly removed from a cylinder coaxial with the z axis so that the vacancy distribution was uniform over the cylinder volume and the average vacancy concentration corresponded to a specified quantity $\langle C_v\rangle$. A two-dimensional thermal spike was introduced at time $t=0$ with a uniform temperature in the cylinder volume. In the calculations the initial radius of the thermal spike, $R_{\rm TS}$, was equal to the radius of the depleted zone, $R_{\rm DZ}$. The initial temperature $T_{\rm th}$ was a variable parameter of the model and varied from 1500 to 8000 K. To analyze the collapse process in the depleted zone, the z projection of all movable atoms was constructed at a time when the temperature in the center of the thermal spike had reduced almost to the ambient temperature, which was chosen to be 300 K. In this way the role of the initial parameters of the thermal spike ($T_{\rm th}$) and depleted zone ($R_{\rm DZ}$,$\langle C_v\rangle$) in the collapse of the DZ was investigated.

The EPC was included in the simulations according to the methods proposed in Refs. 10 and 16. The volume of the calculation cell is divided into two regions by the surface of a cylinder coaxial with z and with radius $R=R_{\rm DZ}$. The diffusional approach was used to calculate the spatial temperature distribution of the electrons. This approach is valid only when the mean free path of an electron, $\lambda=r_0T_0/T_i$, satisfies the condition $\lambda\ll R_{\rm DZ}$, where r_0 is the radius of the Wigner-Seitz cell and T_0 is the value of ion temperature T_i at which the electron mean free path is reduced to r_0. To simplify the solution of the system of equations for $T_i(r,t)$ and the electron temperature $T_e(r,t)$,[16] we used a steady-state equation for T_e in order to estimate the spatial temperature distribution in the central cylinder region $0<r<R_{\rm DZ}$:[10]

$$\nabla^2T_e+\frac{9\Theta_D}{\pi^2r_0^2T_0^2}\,T_i(r,t)[T_i(r,t)-\langle T_e\rangle]=0, \tag{1}$$

in which the interaction between the electron and ion systems is described by using the average electron temperature $\langle T_e\rangle$. $T_i(r,t)$ is the ion temperature at the distance r from the thermal spike center, and Θ_D is the Debye temperature. To calculate the ion temperature distribution, the region ($0<r\leqslant R_{\rm DZ}$) was divided into coaxial hollow cylinders with annular thickness a_0 and the average ion temperature was calculated in each cylinder by MD at each time step. The average electron temperature $\langle T_e\rangle$ in the cylinder region $0<r<R_{\rm DZ}$ was calculated by the expression

$$\langle T_e\rangle=\frac{2}{R_{\rm DZ}^2}\int_0^{R_{\rm DZ}}rT_e(r)dr. \tag{2}$$

The initial condition is $T_e(r,0)=T_c$, where T_c is the ambient temperature, and the boundary conditions are written as

$$T_e(r,t)=T_c, \quad r\geqslant R_{\rm DZ} \tag{3}$$

and

$$\left.\frac{\partial T_e}{\partial r}\right|_{(0,t)}=0. \tag{4}$$

The solution of (1) can be written in the form

$$T_e(r,t)=\left[T_c+\int_0^{R_{\rm DZ}}\frac{d\chi}{\chi}\int_0^{\chi}\xi F(\xi,t)d\xi\right]-\int_0^{r}\frac{d\chi}{\chi}\int_0^{\chi}\xi F(\xi,t)d\xi \qquad (0\leqslant r<R_{\rm DZ}), \tag{5}$$

where

$$F(\xi,t)=\frac{9\Theta_D}{\pi^2r_0^2T_0^2}\,T_i(\xi,t)(T_i(\xi,t)-\langle T_e\rangle). \tag{6}$$

To solve the system of equations (1)–(6), we used a numerical method. The steps of the solution include (a) the definition of the ion temperature distribution $T_i(r,t_n)$ within the central cylinder region of the calculation cell, $0<r\leqslant R_{\rm DZ}$, at the time step t_n by the MD calculation; (b) the calculation of the electron temperature distribution in the cylinder region ($0<r\leqslant R_{\rm DZ}$) by the formulas (5) and (6) for some test value of $\langle T_e\rangle$; (c) the calculation of the average electron temperature by (2) using the solution of $T_e(r,t)$ from Eqs. (5) and (6) obtained for the test value of $\langle T_e\rangle$; (d) if the test value of $\langle T_e\rangle$ differs from the calculated average temperature, then another value is selected and the calculations (b) and (c) are repeated until the correct value of $\langle T_e\rangle$ is found. After finishing these steps, the average electron temperature so obtained is used to calculate the ion temperature at the next time step of the MD simulation.

All ionic velocities, defined by a standard iteration scheme, are scaled at time step n by an appropriate amount depending on the local ion and electron temperatures:

$$v_{n+1}=v_n\sqrt{\beta}, \tag{7}$$

where

$$\beta=\frac{T_{n+1}}{T_n}\cong\frac{\langle T_e\rangle_n}{T_{in}}+\left(1-\frac{\langle T_e\rangle_n}{T_{in}}\right)\exp(-\alpha_e\langle T_e\rangle_n t_0), \tag{8}$$

where $T_n=T_i(r,t_n)$ is the average ion temperature in the cylinder layer between r and $r+a_0$ at the time step n, $\langle T_e\rangle_n$ is the average electron temperature in the region $0<r\leqslant R_{\mathrm{DZ}}$ calculated at time t_n by the method described above, and t_0 is the time step increment. Outside the cylinder region $r\geqslant R_{\mathrm{DZ}}$, the average electron temperature is equal to the ambient temperature: $\langle T_e\rangle_n=T_c$.

The parameter α_e characterizing the strength of the EPC can be estimated by the formula[16]

$$\alpha_e=\left(\frac{3\Theta_D\gamma_e v_f}{\pi^2 r_0 C_p\rho T_0}\right), \tag{9}$$

where γ_e is the coefficient of the electron heat capacity per unit volume, v_f is the Fermi velocity, ρ is the density, and C_p is the specific heat capacity. For Cu and Ni the values of α_e were selected as 1.0×10^9 and 3.3×10^{10} $\mathrm{s^{-1}\,K^{-1}}$, respectively.[11]

III. RESULTS

A. Copper

From the estimates obtained with the hybrid model,[11] the initial values of the parameter $\langle C_v\rangle$ were selected in the range 3–7 at. % and the radius R_{DZ} was varied in the interval $(2-6)a_0$. For these parameters the number of vacancies, N_v, in the DZ changed from 4 to 129.

A typical atomic projection along z of the calculation cell containing the melted region at time $t=100t_0$ is shown in Fig. 1(a). The final structure of the cell at the time $2000t_0$ when the temperature in the center of the DZ had fallen to 300 K is plotted in Fig. 1(b). The results shown in Fig. 1 were obtained for $T_{\mathrm{th}}=4000$ K, $R_{\mathrm{DZ}}=6a_0$ and $\langle C_v\rangle=4$ at. %. It is seen that the calculation cell contains a vacancy loop on the (010) plane (horizontal in the figure) with lattice deformation typical of the strain field of an unfaulted loop in a crystalline solid. In the following, all structures of the cell will be referred to as ''collapsed'' if they include any type of vacancy dislocation loop or similar extended defect containing stacking faults. The symmetry of the cell restricts the collapsed defect geometry in comparison with full 3D relaxation, and so in this work the type of vacancy cluster is not identified precisely and only the conditions for the formation of collapsed structure have been analyzed.

The atomic structure of the cell was analyzed early in the thermal spike cooling in all cases, and it was established that there is a connection between creation of a final collapsed structure and melting of the DZ. It was noticed that melted zones can produce the collapsed structures for $\langle C_v\rangle\geqslant3$ at. %. However, melting is not the only requirement for collapse. We performed a few calculations for $R_{\mathrm{DZ}}=6a_0$ and

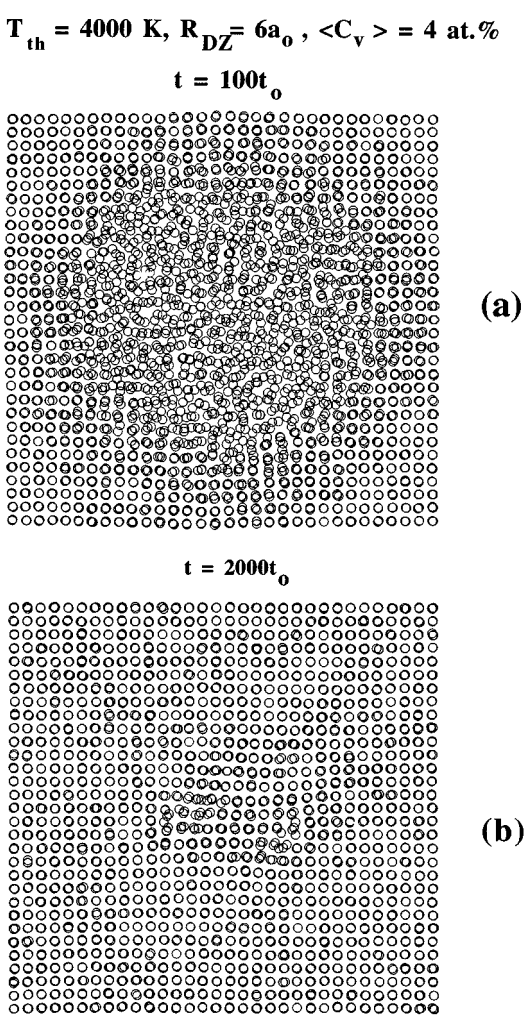

FIG. 1. [001] projection of positions of atoms of the central part of the MD cell at the (a) beginning ($t=100t_0$) and (b) end ($t=2000t_0$) of the thermal spike. The initial concentration and temperature of the DZ were 4 at. % and 4000 K, respectively, and its diameter was $6a_0$.

$T_{\mathrm{th}}=5000$ K and found that the zones having $\langle C_v\rangle=1$ at. % were melted, but the final structure did not consist of a collapsed vacancy cluster.

The dependence on R_{DZ} of the initial temperature T_{th} from which collapsed structures are formed is shown in Fig. 2 for two different values of the parameter $\langle C_v\rangle$. (For the stake of clarity, we have not included all the calculated data in the figure.) The number of vacancies, N_v, for different values of $\langle C_v\rangle$ is indicated by the figures below the curves. The behavior of the curves in Fig. 2 demonstrates the strong sensitivity of the collapse process to the radius of the DZ and number of vacancies in it. Reducing the value of $\langle C_v\rangle$ shifts the curve separating the ''collapse'' and ''no-collapse'' regions to higher temperatures. For $R_{\mathrm{DZ}}>(5-6)a_0$ there is a saturation in the behavior of the curves and the level of the critical temperature is a function of $\langle C_v\rangle$. For $\langle C_v\rangle=7$ at. % and $R_{\mathrm{DZ}}>4a_0$, small 3D vacancy clusters (voids) were observed in the cell for initial temperatures of about 1500–1700 K, and increasing the temperature up to 2000 K was found to lead to the formation of the collapsed structure. For $\langle C_v\rangle=3$ at. % and $R_{\mathrm{DZ}}=6a_0$, the formation of collapsed

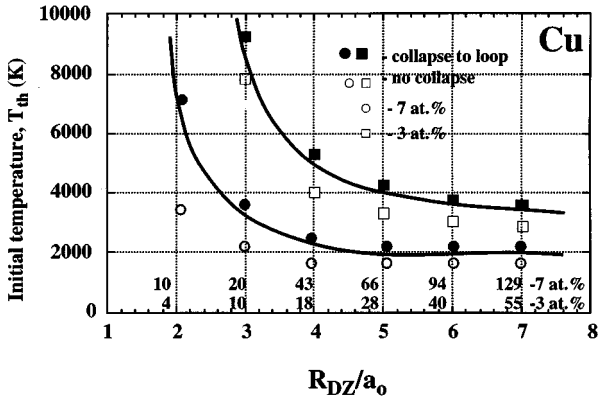

FIG. 2. Results showing the outcome at the end of the thermal spike as a function of initial spike temperature, zone size, and initial average concentration of vacancies in the DZ. Open symbols are the conditions where collapsed vacancy clusters are not produced. Small 3D vacancy clusters (voids) may be sometimes detected in the temperature interval between the open and solid marks. The solid symbols and line show the temperature region above which the DZ melts and then collapses on solidification into a vacancy loop or stacking fault defect.

structure is possible only for initial temperatures above 3500 K and this temperature is seen to increase when the radius of the DZ decreases.

We considered different values of $\langle C_v \rangle$ starting from 3 at. %, but in a real cascade the formation of a DZ with such a high level of average concentration in the melt is possible only at the final stage of the thermal spike. In a real cascade there is a connection between the average temperature $\langle T \rangle$ and the average concentration of vacancies, $\langle C_v \rangle$, in the melt. To establish this connection we used the hybrid model[11] to simulate 50 cascades in a foil of Cu irradiated by 30-keV Cu^+ ions. After melting, a cascade region was found to have a complicated structure containing spatially distinct melted zones: We shall refer to these as "subzones." The values of $\langle T \rangle$ and $\langle C_v \rangle$ were monitored at each time step in each melted subzone, and the results are presented in Fig. 3 as series of curves, each curve representing one molten subzone. Two horizontal lines in Fig. 3 show the region of concentration which the hybrid model showed has to be achieved to initiate collapse. The distribution of the population of molten zones that achieve a concentration 3 at. % is shown as a function of the average temperature in Fig. 4. It is seen that there is a small percentage of zones that attains an average temperature in the interval 3000–6000 K, but the main part of the population is located between the melting temperature and 3000 K.

To plot this histogram all melted zones were included, independent of their size and number vacancies, whereas according to the calculations presented in Fig. 2, the smaller the zone size, the higher the temperature that has to be introduced to initiate collapse. The functions in Fig. 2 can be used to predict the behavior of the melted zones during cooling in the thermal spike. Figure 5 is the data in Fig. 2 replotted to show the initial spike temperature in the melt as a function of the average number of vacancies in the DZ for $\langle C_v \rangle$=3 and 4

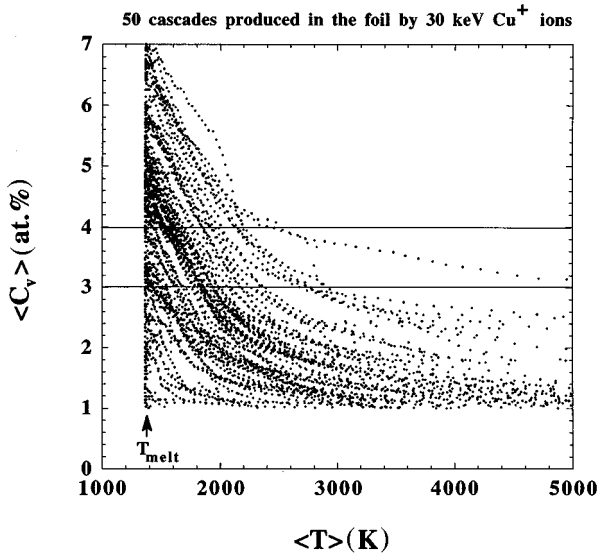

FIG. 3. The dependence of the average concentration of the vacancies, $\langle C_v \rangle$, on the average temperature $\langle T \rangle$ in the melted region of 50 cascades generated by 30-keV Cu^+ ions as simulated in a copper foil by the hybrid model (Ref. 11). Each sequence of points represents the change of $\langle C_v \rangle$ and $\langle T \rangle$ with time for one melted subzone. For the sake of clarity, the parts of curves for $\langle C_v \rangle$ less than 1 at. % are not plotted. Two horizontal lines show the region of concentration which the hybrid model demonstrates has to be achieved to initiate cascade collapse.

at. %. The temperature interval 1500–3000 K, which is identified in Fig. 4 as being associated with the dominant population of zones, is indicated in this figure also. Thus, for most zones of the population to achieve the concentration 3–4 at. %, it is necessary for them to have more than 50–60 vacancies for $\langle C_v \rangle$=4 at. % or 70–80 vacancies for $\langle C_v \rangle$=3 at. %. Zones with this number of vacancies can collapse when the average concentration of vacancies in the melt achieves the level 3–4 at. %. The zones in this temperature interval with fewer vacancies crystallize without collapse.

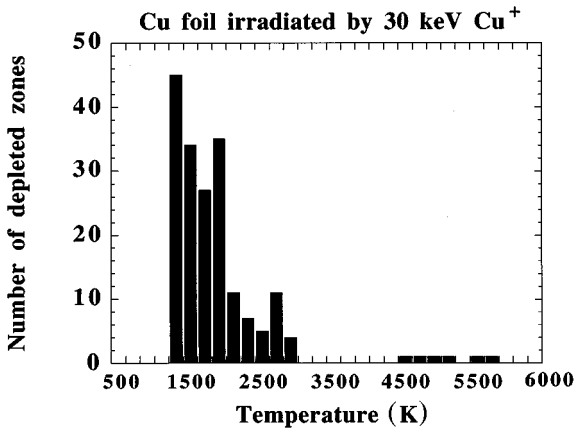

FIG. 4. Distribution of the population of molten subzones that achieve a vacancy concentration of 3 at. % is shown as a function of the average temperature in the melt using the data presented in Fig. 3.

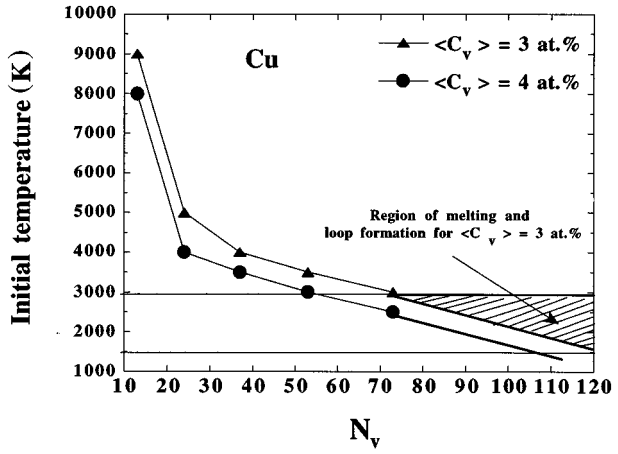

FIG. 5. Initial average temperature in the melted subzone as a function of average number of vacancies in the depleted zone for $\langle C_v \rangle = 3$ and 4 at. % in copper. It is seen that zones in the shaded region can collapse for $\langle C_v \rangle = 3$ at. %.

B. Nickel

The strong EPC in Ni decreases the average size of the melted region and increases the initial temperature gradient in the melt, and depleted zones with a high level of vacancy concentration are formed under these conditions. It has been shown[11] that, in Ni, $\langle C_v \rangle$ can achieve values of more than 20 at. % at the end of the thermal spike stage. This high concentration of vacancies is accompanied by a reduction of the molten zone lifetime. The rapid decrease of the temperature in the melt influences the final structure of the DZ, which, as we have indicated earlier,[10] can transform into a vacancy-rich solid with an irregular structure. In this paper an in-depth examination of this mechanism has been undertaken using the simplified two-dimensional model of the thermal spike and MD code.

The structure of the cell at the beginning of the cooling stage ($t = 100 t_0$) is shown in Fig. 6(a) for the initial values of $T_{\rm th}$ and $R_{\rm DZ}$ equal to 5000 K and $2a_0$, respectively. The positions of atoms in the (001) cross section at the time $2000 t_0$ are shown in Figs. 6(b)–6(e) for different values of $\langle C_v \rangle$ in the range 15–25 at. %. The vacancy concentration for this cylindrical region is defined as the ratio of the number of atoms removed to the number of atoms in the same region for a perfect crystal. It is seen that for $\langle C_v \rangle \leqslant 22$ at. % the final structure of the calculation cell may consist of either a 3D cluster with ordered structure inside it [Fig. 6(c)] or a vacancy loop [Figs. 6(b)–6(d)]. The cluster in Fig. 6(c) includes a surface of stacking faults with irregular shape, and the mechanism of its formation is possibly analogous to that of the stacking fault tetrahedron (SFT). The final structure of the melted zone for $\langle C_v \rangle = 25$ at. % [Fig. 6(e)] has not crystallized completely and has an amorphous core of almost the same size as the initial melted region [Fig. 6(a)].

Calculations of this sort were conducted for $T_{\rm th} = 5000$ K and different sizes of the DZ in the range of $(1.5–5.5)a_0$. About five events were simulated for each size, and variability was introduced by different initial velocity distributions in the heated region. The results are summarized in Fig. 7. The figure demonstrates that for a system with strong EPC the combination of the initial parameters $R_{\rm DZ}$ and $\langle C_v \rangle$ influences the final structure of the DZ after its melting and solidification. For $\langle C_v \rangle < 20$ at. % the melted zones with a size $\geqslant 3a_0$ crytsallize and form 3D vacancy clusters having a structure similar to the SFT. Increasing the initial concentration to up to 25 at. % or more leads to the formation of the irregular amorphouslike structure. Decreasing the size of the DZ (to less than $3a_0$) increases the value of $\langle C_v \rangle$ at which the amorphization takes place. For a very small size (of about $1.5a_0$), the concentration has to be more than 40 at. % to produce the disordered structure. According to our calculations,[11] such concentrations are not achievable in a real cascade in Ni, which means that in spite of the fast cooling there is a critical size of the DZ, represented by $N_v^{\rm am}$, for production of the amorphous core. For $R_{\rm DZ} = 1.5a_0$ and $\langle C_v \rangle = 25$ at. %, this critical size is equal to 25 vacancies.

To examine the influence of the initial parameters on the formation of an amorphous core in the DZ in Ni, we have considered different values of initial spike temperature $T_{\rm th}$ and EPC parameter α_e, and curves similar to that in Fig. 7 were obtained for $T_{\rm th}$ in the range 3000–5000 K. Decreasing the power of EPC by decreasing the value of α_e by a factor of 2 did not influence the formation of the amorphous region since melting occurred in all the zones and the cooling was fast enough to freeze the disordered liquid structure. However, increasing the value of α_e by 2 was found to lead to a situation when the DZ was not melted and an amorphous core was not formed. This situation is similar to the results discussed below for Cu with artificially strong EPC and Fe.

For comparison, a simulation of Cu, but with parameters $\langle C_v \rangle = 25$ at. %, $T_{\rm th} = 5000$ K, $R_{\rm DZ} = 6a_0$, and $\alpha_e = 3.3 \times 10^{10}$ $\rm s^{-1}\,K^{-1}$, appropriate for Ni, was undertaken. We found that the DZ did not melt and the final structure was obtained without formation of an amorphous core. Usually the DZ transformed into a 3D stacking fault defect under the influence of the thermal agitation of the lattice. Only after decreasing the value of α_e by 2 did the DZ melt and change into the amorphous structure.

C. bcc iron

As another example of a system with strong EPC, bcc iron has been investigated. It is known that iron has stronger EPC than Ni,[5,6] but an accurate value of α_e is not available at the moment. For this reason we used the same value of α_e as for Ni, but note that in reality the cooling rate of the thermal spike in iron is expected to be faster. The main result of our calculation demonstrated that, for any reasonable values of the main input parameters of the thermal spike ($T_{\rm th}$, $R_{\rm DZ}$) and α_e as for Ni, melting does not occur. This is similar to the situation described above for Cu with artificially high α_e. The MD simulations revealed that the DZ in Fe does not melt, but can transform to a vacancy loop under the influence of the thermal agitation of the lattice if the initial concentration of vacancies is more than 20 at. %. It is probable that in reality cascades in Fe can collapse without DZ melting only when the irradiation conditions produce DZs with a high enough concentration of vacancies, for instance, under heavy ion irradiation, as found experimentally.[17] When the value of α_e in the MD model of iron was halved, the DZ melted in the thermal spike and an amorphous structure was obtained for $\langle C_v \rangle > 20$ at. % (Fig. 8).

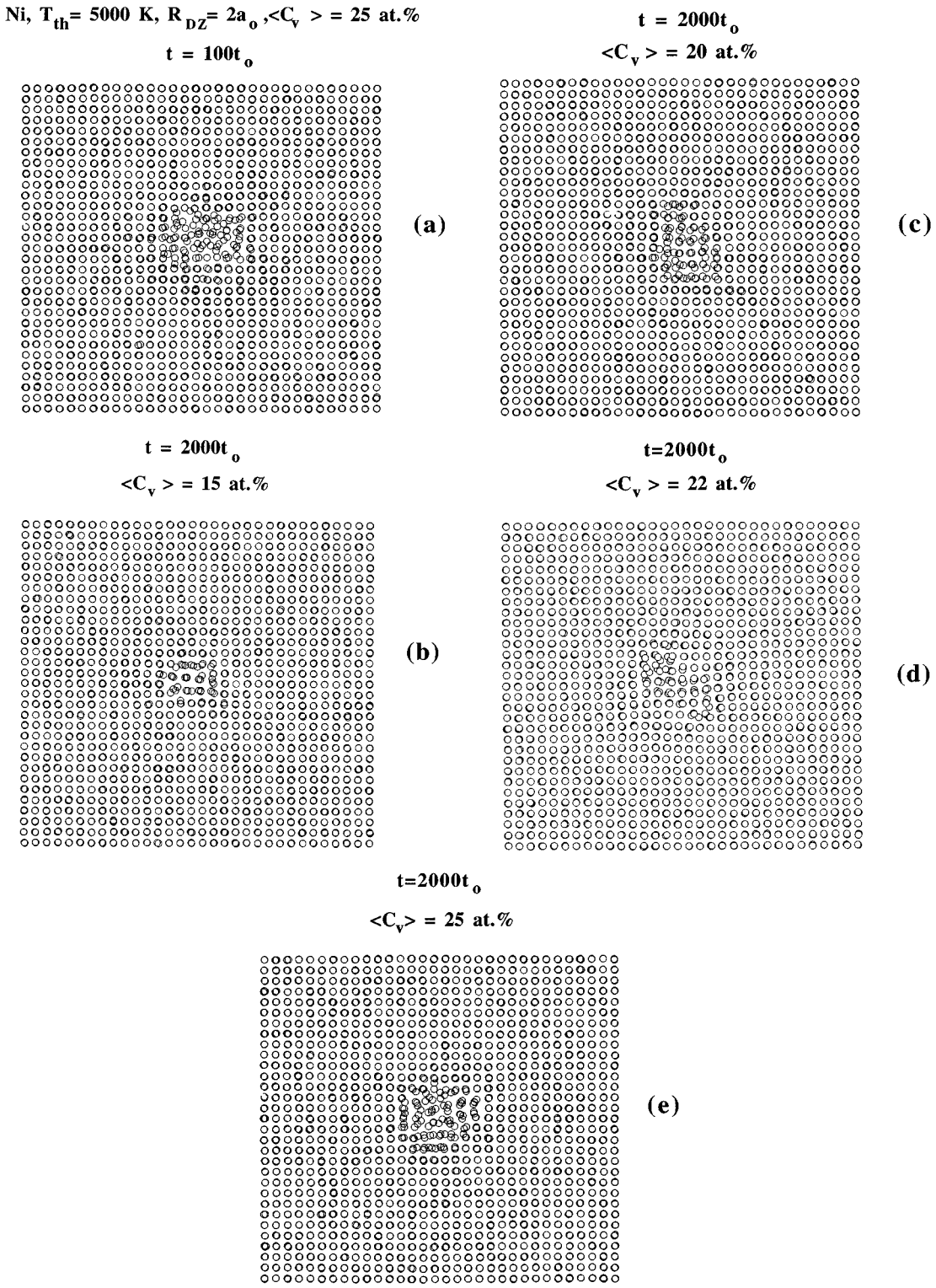

FIG. 6. [001] projections of atoms of the central part of the calculation cell at the (a) beginning and (b)–(e) end of the thermal spike in Ni. The initial average concentration of vacancies was (b) 15 at. %, (c) 20 at. %, (d), 22 at. %, and (e) 25 at. %.

IV. DISCUSSION

Earlier[10,11] we proposed a model for the nucleation of collapsed vacancy clusters in irradiated metals. According to this, a vacancy loop is nucleated in the region of a cascade, which, after melting and recrystallization, reaches the critical concentration of vacancies, C_v^{cr}. The model included parameters which can be defined from comparison of calculated values of loop size and yield with experimental data. The model was used to predict the yield and mean size of vacancy loops in ion-irradiated Cu, Ni, and their alloys. We demonstrated that in Cu irradiated by 30-keV Cu^+ ions the melted DZ collapses into a vacancy loop after crystallization if the average concentration of vacancies in that zone is more than 3–4 at. %. Experimentally, there is a saturation in the

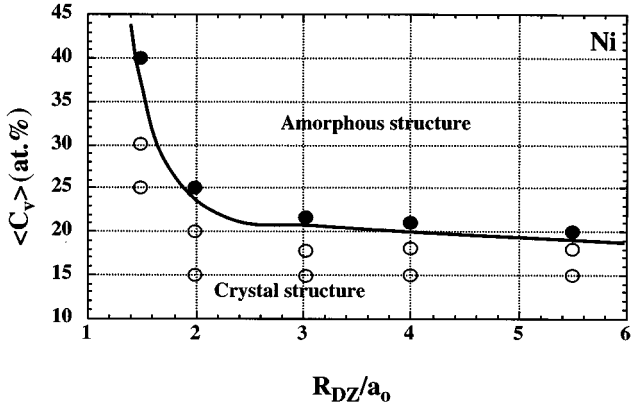

FIG. 7. Curve represents the boundary between the crystalline and amorphouslike regions which are formed in Ni after the thermal spike in a DZ with $T_{\rm th}=5000$ K. Similar results are obtained for all initial temperatures in the range 3000–5000 K.

loop yield with increasing ion energy, but if it is supposed that all zones with $\langle C_v\rangle=3$–4 at. % can collapse to vacancy loops, the calculated yield saturates at a level of 0.8–0.85, which is higher than the observed value of 0.5. To achieve better agreement between calculation and experiment, we included in the model the additional parameter $N_v^{\rm cr}$ by assuming that only zones containing an average number of vacancies of more than $N_v^{\rm cr}$ can produce a visible loop. By increasing the value of $N_v^{\rm cr}$ from 30 to 60, it was possible to reduce the calculated yield from 0.8 to 0.6, in reasonable agreement with experiment.

In the present work we have aimed to give a physical explanation of the parameter $N_v^{\rm cr}$ by using MD simulations to study the collapse processes in a DZ. The approach of Finnis *et al.*[16] has been incorporated in the thermal spike model to take the EPC into account in a manageable way. These simulations allow us to conclude that there is a direct connection between the melting of depleted zones in Cu and their collapse to form vacancy loops for $\langle C_v\rangle\geqslant 3$ at. %. The vacancy loop production is sensitive to the size of the DZ at a given fixed level of $\langle C_v\rangle$. A decrease in the size of the DZ increases the value of the initial spike temperature required to initiate collapse. Curves of the initial temperature of the zones that collapse has been derived as a function of $R_{\rm DZ}$, $\langle C_v\rangle$, and $T_{\rm th}$ for Cu (Fig. 2), and it provides a qualitative understanding of the mechanism underlying the influence of DZ size on the collapse process in a real cascade. To explain this consider the mechanism of DZ formation based on the hybrid model.[11] At the beginning of the thermal spike, the temperature is high enough to stimulate melting of part of the DZ. During cooling, the size of the melted zone decreases, but the density of the melt is decreased under the influence of the "vacancy sweeping mechanism."[9,10] When the size of the melt is decreased to some critical value, crystallization takes place and a zone with an average concentration of vacancies, $\langle C_v\rangle$, is formed. It is reasonable to assume that the initial temperature of a zone which can collapse is a function of DZ size or number of vacancies located within the melt, N_v. We have demonstrated in Ref. 11 that the critical concentration for collapse, $C_v^{\rm cr}$, is achievable only at the end of the thermal spike, when the average temperature is

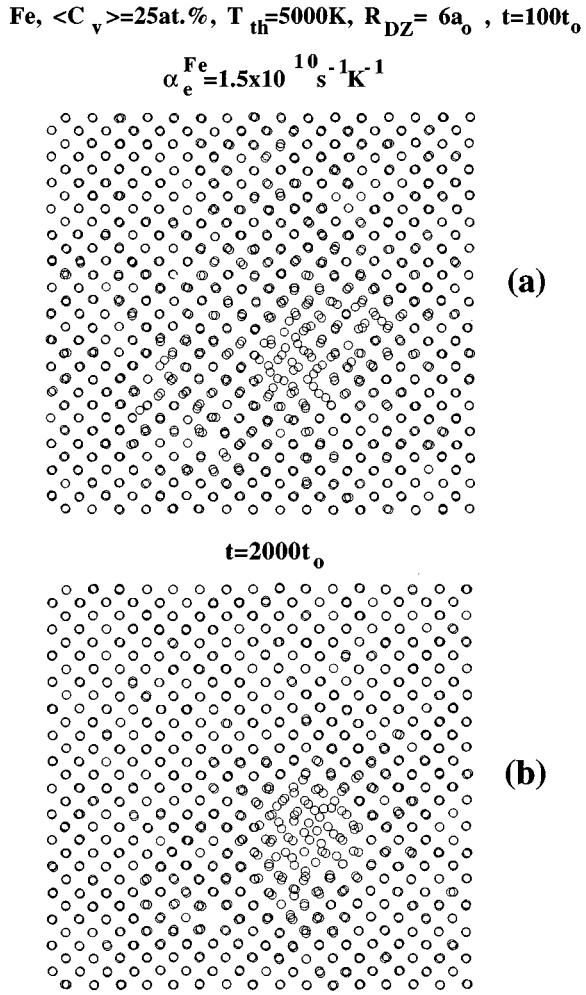

FIG. 8. [001] projections of position of atoms of the central part of the MD cell at (a) the beginning and (b) end of the thermal spike in Fe. To melt the DZ in iron and produce the amorphous structure, the strength of the EPC has been halved compared with that for Ni.

within the range from the melting temperature $T_{\rm melt}$ to 3000 K. [This ignores the small fraction of zones which can achieve this concentration for higher temperature (Fig. 4).] The crystallization of a DZ of small size may happen before $\langle C_v\rangle$ achieves the value $C_v^{\rm cr}$, and the DZ would not then collapse to a vacancy loop. We performed 50 simulations of cascades in copper and obtained the dependence of average temperature on $\langle C_v\rangle$ in the melt (Sec. III A). The results have been analyzed within the scope of our understanding of the influence of DZ size on the collapse process. The comparison has shown that a DZ has to contain a minimum of 50–60 vacancies for $C_v^{\rm cr}=3$ at. % and 70–80 for $C_v^{\rm cr}=4$ at. % to produce a loop. These values are in very good agreement with the parameter $N_v^{\rm cr}$ extracted in our earlier work[11] from the experiment data.

In Ni the strong EPC increases the final value of $\langle C_v\rangle$ by several times compared to the values achieved in copper. To describe the behavior of the DZ with a high concentration of vacancies in Ni, we previously proposed the idea[10] that the core of a cascade with a high level of vacancy concentration is unlikely to recrystallize completely and will solidify instead to a semiamorphous zone that cannot collapse to form a loop. The additional parameters $C_v^{\rm am}$ and $N_v^{\rm am}$ were incor-

porated into the hybrid model to simulate the behavior of metals under the influence of strong EPC. By fitting the model calculations to the experimental data, values of $C_v^{\mathrm{am}} = 21-22$ at. % and $N_v^{\mathrm{am}} = 20-25$ vacancies were derived.

In this paper we have investigated the influence of strong EPC on the final structure of a DZ in Ni using MD simulations with a cylindrical thermal spike and shown that a melted DZ with an average concentration of vacancies of more than 20 at. % and size larger than $(2-3)a_0$ solidifies to a solid with a high concentration of vacancies and highly disordered structure, i.e., a zone with some amorphous character. The final structure of a DZ with average concentration less than 25 at. % after solidification usually consists of a vacancy loop; i.e., collapse occurs. In the range 20–22 at. %, the DZ transforms into a configuration which consists of a 3D cluster of irregular shape formed from the surfaces of stacking fault defects or vacancy loops. For a DZ of very small size ($<2a_0$), the amorphization does not take place even for high initial temperature. Analysis of the heated structure shows that there is a strong correlation of the position of atoms in a small DZ. The atoms vibrate near the crystal sites, and during the cooling, this overheated crystallike region returns to the crystal structure rather than an amorphous one. The critical number of vacancies in a zone which cannot become amorphous is 20–25, which is very close to the value obtained from comparison of the calculations using the hybrid model with experiment.[11] The results of the MD simulations support our earlier conclusion that the strong EPC in Ni has a powerful influence on the loop yield in displacement cascades through the formation of the amorphouslike core in the melted DZ.

We have considered iron as another example of a system with strong electron-phonon coupling but different type of lattice. Using the same value of the EPC parameter α_e as for Ni, it has been demonstrated that the DZ cannot melt in iron. The estimation of the true EPC for this metal[5] shows that α_e is actually higher than in Ni. This means that in reality DZ melting is a less likely process in Fe than in Ni and nucleation of a vacancy loop is possible only for special cases in which the DZ has high fluctuations of temperature and vacancy concentration. For instance, at a high initial vacancy concentration of 20 at. % or more the transformation of a DZ into a collapsed vacancy configuration can take place without melting. The formation of a DZ with such a high level of vacancy concentration without melting in iron is possible only in cascades generated, for instance, by heavy ions such as W^+, a conclusion consistent with experiment.[17]

It is not clear why Ni melts but Fe does not. One possible factor is the higher stiffness of the atomic bonds, as displayed in the elastic constant and phonon spectra. Since the high temperature of the thermal spike only exists for a very short time (comparable with the atomic vibration period) for strong EPC, the difference in vibration frequency may allow Ni to form the liquid state, whereas Fe requires more time to disorder.

V. CONCLUSIONS

(1) A model of vacancy cluster nucleation in a displacement cascade has been proposed, based on the MD simulations of the thermal stage of cascade development. The electron-phonon coupling has been included in the model simply by the procedure of scaling the ion velocities to imitate a viscous force acting on a moving atom in accordance with the approach of Finnis *et al.*[16]

(2) The model has been used to analyze the influence on vacancy loop nucleation of the size and average vacancy concentration of the depleted zone, the initial average temperature in the thermal spike, and the strength of EPC.

(3) It has been demonstrated that there is a strong correlation between the melting of a depleted zone and the formation of a loop as the zone crystallizes on solidification when the value of the average concentration of vacancies in the melt is $\geqslant 3$ at. %.

(4) For copper the temperature at which a DZ collapses is a function of zone size and number of vacancies inside it. The function has been derived and used to obtain the critical number of vacancies to nucleate loops in Cu irradiated by 30-keV Cu^+ ions. The result is in good agreement with the number extracted from experiment in Ref. 11.

(5) The melting and solidification of a DZ in Ni under the influence of strong electron-phonon coupling has been analyzed. It has been found that melted zones with a high concentration of vacancies (more than 20 at. %) can be achieved, but they may solidify into an amorphouslike structure. However, this process is possible only for zones with a size more than $(1.5-2.0)a_0$, where a_0 is the lattice parameter. These findings explain the low vacancy loop yield in nickel.

(6) DZ cooling in bcc iron has been simulated using the same EPC as in Ni and similar zone parameters. It has been shown that there is a low probability of zone melting. Loop formation in an unmelted DZ is possible when the zone contains an initially high concentration of vacancies. Such zones may be formed at the dynamical stage of cascade evolution during irradiation by heavy ions.

ACKNOWLEDGMENTS

We would like to thank Dr. A. G. Mikhin for useful discussions and critical comments on the results of this research. V.G.K. acknowledges the hospitality of the University of Liverpool. The work was supported by INTAS Grant No. INTAS-93-3454.

[1] T. Diaz de la Rubia and M. W. Guinan, Mater. Res. Forum **97-99**, 23 (1992).

[2] D. J. Bacon and T. Diaz de la Rubia, J. Nucl. Mater. **216**, 275 (1994).

[3] V. G. Kapinos and P. A. Platonov, Phys. Status Solidi A **90**, 291 (1985).

[4] H. van Swygenhoven and A. Caro, Phys. Rev. Lett. **70**, 2098 (1993).

[5] D. K. Tappin, I. M. Robertson, and M. A. Kirk, Philos. Mag. A **70**, 463 (1994).

[6] I. M. Robertson, D. K. Tappin, and M. A. Kirk, Philos. Mag. A **68**, 843 (1993).

[7] K. Morishita, H. L. Heinisch, S. Ishino, and N. Sekimura, J. Nucl. Mater. **212-215**, 198 (1994).
[8] M. Alurralde, A. Caro, and M. Victoria, J. Nucl. Mater. **183**, 33 (1991).
[9] V. G. Kapinos and D. J. Bacon, Philos. Mag. A **68**, 1165 (1993).
[10] V. G. Kapinos and D. J. Bacon, Phys. Rev. B **50**, 13 194 (1994).
[11] V. G. Kapinos and D. J. Bacon, Phys. Rev. B **52**, 4029 (1995).
[12] M. Caro, A. Ardelea, and A. Caro, J. Mater. Res. **5**, 2652 (1990).
[13] M. T. Robinson, computer code MARLOWE, Oak Ridge National Laboratory, 1992.
[14] G. J. Ackland and V. Vitek, Phys. Rev. B **41**, 10 324 (1990); V. Vitek, G. J. Ackland, and J. Cserti, in *Alloy Phase Stability and Design*, edited by G. M. Stocks, D. P. Pope, and A. F. Giamei, MRS Symposia Proceedings No. 186 (Material Research Society, Pittsburgh, 1991) p. 227; Fe potential: G. J. Ackland, D. J. Bacon, and A. F. Calder (unpublished).
[15] Cu potential: H. F. Deng and D. J. Bacon, Phys. Rev. B **48**, 10 022 (1993); Ni potential: F. Gao and D. J. Bacon, Philos. Mag. A **67**, 275 (1993).
[16] M. W. Finnis, P. Agnew, and A. J. E. Foreman, Phys. Rev. B **44**, 567 (1991).
[17] M. L. Jenkins, C. A. English, and B. L. Eyre, Philos. Mag. **38**, 97 (1978).